Proceedings of the 1998 IEEE
International Conference on Robotics & Automation
Leuven, Belgium • May 1998

A Comparative Study of Vision-Based Lateral Control Strategies for Autonomous Highway Driving

J. Košecká, R. Blasi, C. J. Taylor and J. Malik
Department of Electrical Engineering and Computer Sciences
University of California at Berkeley
Berkeley, CA 947, USA.
email: janak,blasirs,camillo,malik@cs.berkeley.edu

Abstract

This paper will present the results of a comparative study of a set of vision-based control strategies that have been applied to the problem of steering an autonomous vehicle along a highway. The aim of this work has been to further our understanding of the characteristics of various control laws that could be applied to this problem with a view to making informed design decisions. The control strategies that we explored include a lead lag control law, a full-state linear controller and input-output linearizing control law. Each of these control strategies was implemented and tested on our experimental vehicle, a Honda Accord LX, both with and without a curvature feedforward component.

1 Introduction

With the increasing speeds of modern microprocessors it has become ever more common for computer vision algorithms to find application in real-time control tasks. In particular, the problem of steering an autonomous vehicle along a highway using the output from one or more video cameras mounted inside the vehicle has been a popular target for researchers around the world and a number of groups have demonstrated impressive results on this control task. Dickmanns et. al. [2] developed a system that drove autonomously on the German Autobahn as early as 1985. The Navlab project at CMU has produced a number of successful visually guided autonomous vehicle systems. Other research groups include Ozguner et. al. at Ohio State [10], Broggi et al at the Universita' di Parma, Raviv and Herman at the National Institute of Standards [12] and Lockheed-Martin.

The goal of our research efforts in this field has been to understand the fundamental characteristics of this vision based control problem and to use this knowledge to design better control strategies. In [7] we presented an analysis of the problem of vision-based lateral control and investigated the effects of changing various important system parameters like the vehicle velocity, the lookahead range of the vision sensor and the processing delay associated with the perception and control system. We also described a static feedback strategy that enabled us to perform the lateral control task at highway speeds. We were able to verify the accuracy and efficacy of our modelling and control techniques on our experimental vehicle platform, a Honda Accord LX.

In this paper we present the results of a series of experiments that were designed to provide a systematic comparison of a number of control strategies. The aim of this work has been to further our understanding of the characteristics of various control laws that could be applied to this problem with a view to making informed design decisions. The control strategies that we explored include a lead lag control law, a full-state linear controller and input-output linearizing control law. Each of these control strategies was implemented and tested both with and without a curvature feedforward component.

Section 2 of this paper presents the basic equations that we have used to model the dynamics of our vehicle and our sensing system. Section 3 describes the design of the observer that we use to estimate the states of our system and the curvature of the roadway. Section 4 describes the various control strategies that we implemented on our experimental platform and section 5 presents the results of the experiments that we carried out with these controllers. Section 6 contains the conclusions that we have drawn from these experiments.

2 Modeling and Analysis

The dynamics of a passenger vehicle can be described by a detailed 6-DOF nonlinear model [11].

0-7803-4300-x-5/98 $10.00 © 1998 IEEE

Since it is possible to decouple the longitudinal and lateral dynamics, a linearized model of the lateral vehicle dynamics is used for controller design. The linearized model of the vehicle retains only lateral and yaw dynamics, assumes small steering angles and a linear tire model, and is parameterized by the current longitudinal velocity. Coupling the two front wheels and two rear wheels together, the resulting bicycle model (Figure 1) is described by the following variables and parameters:

$\boldsymbol{v}$ linear velocity vector (v_x, v_y), v_x denotes speed

α_f, α_r side slip angles of the front and rear tires

$\dot{\psi}$ yaw rate

δ_f front wheel steering angle

δ commanded steering angle

m total mass of the vehicle

I_ψ total inertia vehicle around center of gravity (CG)

l_f, l_r distance of the front and rear axles from the CG

l distance between the front and the rear axle $l_f + l_r$

c_f, c_r cornering stiffness of the front and rear tires.

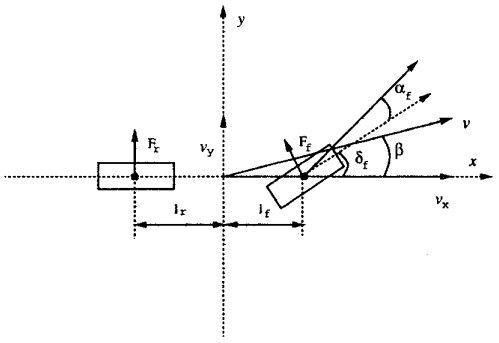

Figure 1: The motion of the vehicle is characterized by its velocity $\boldsymbol{v} = (v_x, v_y)$ expressed in the vehicle's inertial frame of reference and its yaw rate $\dot{\psi}$. The forces acting on the front and rear wheels are F_f and F_r, respectively.

The lateral dynamics equations are obtained by computing the net lateral force and torque acting on the vehicle following Newton-Euler equations [1] and choosing $\dot{\psi}$ and v_y, as state variables. The state equations have the following form:

$$\begin{bmatrix} \dot{v}_y \\ \ddot{\psi} \end{bmatrix} = \begin{bmatrix} -\frac{a_1}{m v_x} & \frac{-m v_x^2 + a_2}{m v_x} \\ \frac{a_3}{I_\psi v_x} & -\frac{a_4}{I_\psi v_x} \end{bmatrix} \begin{bmatrix} v_y \\ \dot{\psi} \end{bmatrix} + \begin{bmatrix} b_1 \\ b_2 \end{bmatrix} \delta_f \quad (1)$$

where $a_1 = c_f + c_r$, $a_2 = c_r l_r - c_f l_f$, $a_3 = -l_f c_f + l_r c_r$, $a_4 = l_f^2 c_f + l_r^2 c_r$, $b_1 = \frac{c_f}{m}$ and $b_2 = \frac{l_f c_f}{I_\psi}$. The additional measurements provided by the vision system (see Figure 2) are:

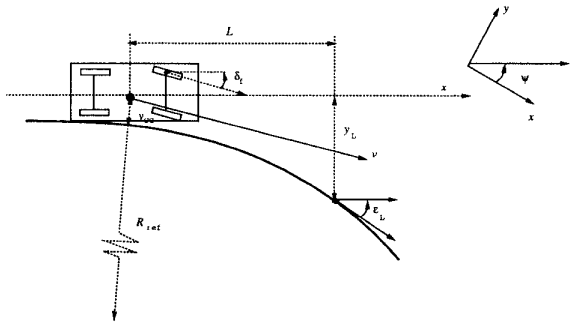

Figure 2: The vision system estimates the offset from the centerline y_L and the angle between the road tangent and heading of the vehicle ε_L at some lookahead distance L.

y_L the offset from the centerline at the lookahead,

ε_L the angle between the tangent to the road and the vehicle orientation

L denotes the lookahead distance of the vision system. The equations capturing the evolution of these measurements due to the motion of the car and changes in the road geometry are:

$$\dot{y}_L = v_x\, \varepsilon_L - v_y - \dot{\psi} L \quad (2)$$

$$\dot{\varepsilon}_L = v_x\, K_L - \dot{\psi} \quad (3)$$

We can combine the vehicle lateral dynamics and the vision dynamics into a single dynamical system of the form:

$$\dot{\boldsymbol{x}} = A\,\boldsymbol{x} + B\,\boldsymbol{u} + E\,\boldsymbol{w}$$
$$\boldsymbol{y} = C\,\boldsymbol{x}$$

with the state vector $\boldsymbol{x} = [v_y, \dot{\psi}, y_L, \varepsilon_L]^T$, the output $y = [\dot{\psi}, y_L, \varepsilon_L]^T$ and control input $\boldsymbol{u} = \delta_f$. The road curvature K_L enters the model as an exogenous disturbance signal $\boldsymbol{w} = K_L$.

A block diagram of the overall system based on the state equations is shown in Figure 3. The transfer function $V_1(\boldsymbol{s})$ between the steering angle δ_f and offset at the lookahead y_L has the following form:

$$V_1(\boldsymbol{s}) = \frac{1}{\boldsymbol{s}^2} \frac{a\boldsymbol{s}^2 + b\boldsymbol{s} + c}{d\boldsymbol{s}^2 + e\boldsymbol{s} + f} \quad (4)$$

where the numerator is a function of both speed and lookahead distance and the denominator is parameterized by the speed of the car. $V_1(\boldsymbol{s})$ can be rewritten according to Figure 3 by singling out the vehicle dynamics in terms of $\ddot{y}_{CG}$ and $\ddot{\psi}$ followed by the integrating action $1/s^2$:

$$V_1(\boldsymbol{s}) = \frac{1}{\boldsymbol{s}^2}(G(\boldsymbol{s}) + L\,G_2(\boldsymbol{s})) \quad (5)$$

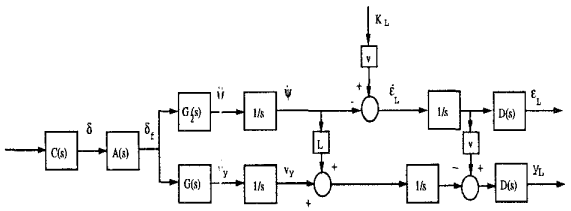

Figure 3: The block diagram of the overall system with the two outputs provided by the vision system.

where $G(s)$ and $G_2(s)$ are transfer functions between steering angle and lateral acceleration and yaw acceleration respectively. The actuator $A(s)$ is modeled as a low pass filter of the commanded steering angle δ and a pure time delay element $D(s) = e^{-T_d s}$ represents the latency T_d of the vision subsystem. In our system $T_d = 0.057$ s. The transfer function $C(s)$ corresponds to the controller to be designed. A more detailed analysis of how the behavior of this dynamic system changes as a function of important system parameters like, lookahead distance, processing delay and vehicle velocity can be found in [7].

3 Vision System

The vision-based lane tracking system used in our experiments is an improved version of the one presented in [13]. This system takes its input from a single forward-looking CCD video camera. It extracts potential lane markers from the input using a template-based scheme. It then finds the best linear fits to the left and right lane markers over a certain lookahead range through a variant of the Hough transform. From these measurements we can compute an estimate for the lateral position and orientation of the vehicle with respect to the roadway at a particular lookahead distance, L.

The vision system is implemented on an array of TMS320C40 digital signal processors which are hosted on the bus of an Intel-based industrial computer. The system processes images from the video camera at a rate of 30 frames per second.

4 Observer Design

In order to estimate the curvature of the roadway we have chosen to implement an observer based on a slightly simplified version of the systems state equations as shown in Equation (6). More specifically, in these equations we have chosen to neglect the vehicles lateral velocity, v_y.

$$\dot{\boldsymbol{x}}' = A'(v_x)\boldsymbol{x}' + B'\dot{\psi}$$

$$\boldsymbol{y}' = C'\boldsymbol{x}' \tag{6}$$

where $\boldsymbol{x}' = [y_L, \varepsilon_L, K_L]^T$, $\boldsymbol{y}' = [y_L, \varepsilon_L]^T$. Note that the state vector $\boldsymbol{x}'$ includes the road curvature K_L. This differential equation can be converted to discrete time in the usual manner by assuming that the yaw rate, $\dot{\psi}$, is constant over the sampling interval T.

$$\boldsymbol{x}'(k+1) = \Phi(v_x)\boldsymbol{x}'(k) + \beta\dot{\psi} \tag{7}$$

Equation (7) allows us to predict how the state of the system will evolve between sampling intervals.

Measurements are obtained from two sources: the vision system provides us with measurements of y_L and ε_L, while the on-board fiber optic gyro provides us with measurements of the yaw rate of the vehicle, $\dot{\psi}$. Our use of the yaw rate sensor measurements is analogous to the way in which information from the proprioceptive system is used in animate vision. The measurement vector $\boldsymbol{y}'$ is used to update an estimate for the state of the system $\hat{\boldsymbol{x}}'$ as shown in the following equation:

$$\hat{\boldsymbol{x}}'^{+}(k) = \hat{\boldsymbol{x}}'^{-}(k) + L(\boldsymbol{y}'(k) - C\hat{\boldsymbol{x}}'^{-}(k)) \tag{8}$$

where $\hat{\boldsymbol{x}}'^{-}(k)$ and $\hat{\boldsymbol{x}}'^{+}(k)$ denote the state estimate before and after the sensor update respectively.

The gain matrix L can be chosen in a number of ways [4], depending on the assumptions one makes about the availability of noise statistics and the criterion one chooses to optimize. In our case, the gain matrix was chosen to minimize the expected error of our estimate in the steady state using the function `dlqe` available in Matlab. The covariances of both the process and measurement noise were estimated by analyzing the data collected by our sensors during trial runs with the vehicle.

5 Controllers

The goal of all of the control schemes presented in the sequel is to regulate the offset at the lookahead, y_L, to zero. Passenger comfort is another important design criterion and this is typically expressed in terms of jerk, corresponding to the rate of change of acceleration. For a comfortable ride no frequency above 0.1-0.5 Hz should be amplified in the path to lateral acceleration [5]. Additional performance criteria may be specified in terms of the maximal allowable offset y_{Lmax} as a response to the step change in curvature and in terms of bandwidth requirements on the transfer function $F(s) = \frac{y_L(s)}{K_L(s)}$.

Lead-lag Control. Previous analysis [7] revealed that at speeds of up to 15 m/s with a lookahead

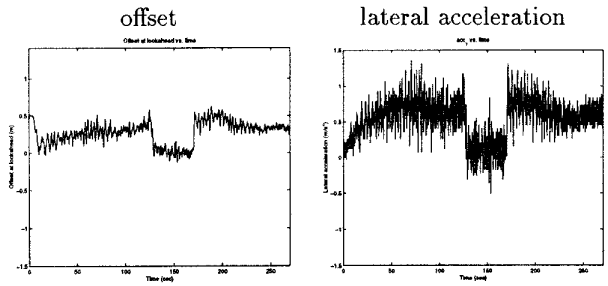

Figure 4: Lead-Lag controller. The offset was measured at the lookahead of 15 m. The performace of the lead-lag controler in terms of offset was superior compared to the other tested strategies.

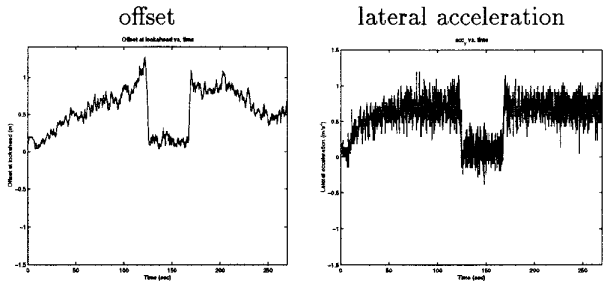

Figure 5: Full State Feedback controller. The offset measured at the look-ahead distance of 6 m results in a less noisy measurements. The lateral acceleration profile degraded towards the end of the run due to the increase in linear velocity.

of around 10 meters one can guarantee satisfactory damping of the closed loop poles of $V_1(s)$ and compensate for the processing delay of the vision system using simple unity feedback control with proportional gain in the forward loop. As the velocity increases, the poles of the transfer function move toward the real axis and become more poorly damped which introduces additional phase lag in the frequency range 0.1-2 Hz. Since further increasing the lookahead does not improve the damping, gain compensation alone cannot achieve satisfactory performance. A natural choice for obtaining an additional phase lead in the frequency range 0.1-2 Hz would be to introduce some derivative action, however, in order to keep the bandwidth low an additional lag term is necessary. One satisfactory lead-lag controller has the following form:

$$C(s) = \frac{0.09s + 0.18}{0.025s^2 + 1.5s + 20} \tag{9}$$

where $C(s)$ is a lead network in series with a single pole. The above controller was designed for a velocity of 30 m/s (108 km/h, 65 mph), a lookahead of 15 m and 60 ms delay. The resulting closed loop system has a bandwidth of 0.45 Hz with a phase lead of 45° at the crossover frequency. A discretized version of the above controller taking into account the 33 ms sampling time of the vision system was used in our experiments. The performance of the controller is in Figure 4.

Since increasing the speed has a destabilizing effect on $V_1(s)$, designing the controller for the highest intended speed guarantees stability at lower speeds and achieves satisfactory ride quality. In order to tighten the tracking performance at lower speeds individual controllers can be designed for various speed ranges and gain scheduling techniques used to interpolate between them.

Full State Feedback. Given that the vehicle can be modeled as a linear dynamical system it seems natural to consider standard full state linear feedback laws of the form $u = Kx$. The controller was designed for velocity of 20 m/s and a lookahead of 6 meters. The gain matrix, K, was then chosen using pole placement techniques such that the two poles of the system that were originally at the origin were moved to a conjugate pair with a damping ratio $\xi = 0.707$ and a natural frequency $\omega_n = 0.989$ rad/s. The other two poles of the system were left unchanged. These pole locations were chosen so that the resulting system would satisfy our step response and bandwidth requirements.

In the resulting linear control law, the gain associated with the lateral velocity term v_y was small so we chose to neglect this component of the controller. Estimates for the remaining state variables, y_L, ε_L, and $\dot{\psi}$ are obtained from our observer and the yaw rate sensor. The offset and lateral acceleration profiles are in Figure 5.

Input-Output Linearization. Input-output linearization is typically used to linearize nonlinear systems by state feedback as described in [6]. The application of this technique to the bicycle model is not, strictly speaking, linearization by state feedback since the bicycle model is already linear. Nonetheless, this technique can be applied to render the model independent of the vehicles longitudinal velocity, v_x. In this case the feedback law has a zero cancelling effect instead of linearizing one and makes the vehicle dynamics poles unobservable. Given the bicycle model in the form $\dot{x} = f(x) + g(x)u$ consider the control law

$$u = \frac{1}{L_g L_f^1 h(x)}(-L_f^2 h(x) + u') \tag{10}$$

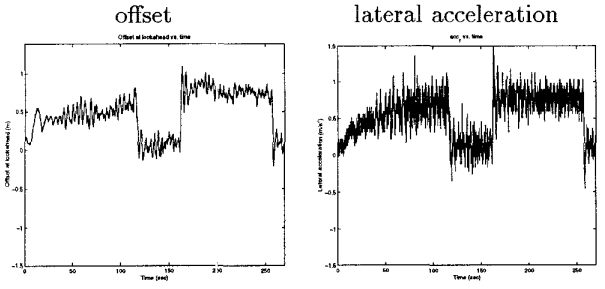

Figure 6: I/O linearized controller. The overshoots during the transitions are noticeable and performance slightly degrades with increasing speed towards the end of the test run.

where L_g^i denotes the i-th Lie derivative along g. For our particular example the control law becomes:

$$u = a\,(u' - \frac{(\frac{La_3}{I_\psi} - \frac{a_1}{m})v_y - (\frac{-La_4}{I_\psi} - \frac{a_2}{m})\dot{\psi}}{v_x})$$

with
constants $a = 1/(-Lb_2 - b_1)$ and $a_1, a_2, a_3, a_4, b_1, b_2$ as defined in Equation 1. Employing this control law yields a second order equation of the form $\ddot{y} = u'$. Once the system has been reduced to this form we can employ the same lead-lag control law described previously to compute u' and stabilize the system as well as obtain the desired performance.

Feedforward Control The steady state steering input, δ_{ref}, that is required to track a reference K_{Lref} can be computed from the state equations by setting $[\dot{v}_y, \ddot{\psi}, \dot{y}_L, \dot{e}_L]^T$ to 0.

$$\delta_{ref} = K_{ref}\,(l - \frac{(l_f c_f - l_r c_r)v_x^2 m}{c_r c_f l}). \qquad (11)$$

This feedforward control component can be added to any of the control schemes that have been described. The feedforward control law allows the system to anticipate changes in curvature ahead of the car and improves the transient behavior of the vehicle when entering and exiting curves (see Figure 7). The effectiveness of the feedforward term will, of course, depend on the quality of the curvature estimates supplied by the observer.

6 Experimental Results

In order to evaluate different feedback and feedforward strategies we implemented them on our experimental vehicle and collected data from a number of trial runs. Our test track was a 7 mile oval and our experiments were run at speeds of approximately 75mph to simulate actual highway conditions. Each experimental trial lasted at least 5 minutes, long enough to explore how each controller fared on the straight sections, the curved sections and the transitions between them. Figures 4, 5, 6 describe performance of individual feedback control strategies and Figure 7 depicts the performance of the curvature estimator and some of the tested control strategies with the feedforward term.

7 Conclusions

The strategy behind the design of the feedback control laws was based on the observation that the behavior of our system was dominated by the two poles at the origin, since the other two poles are well behaved as long as the lookahead distance is large enough. This allowed us to design controllers for the highest intended operating velocity, which would operate satisfactorily in the whole range of lower velocities. However this approach sacrifices some performance criteria at lower velocities.

Our experiments indicate that all three of the feedback control strategies that we implemented provided acceptable performance on the lateral control task with the lead lag control law yielding the best tracking performance of the three. The data also shows that the curvature feedforward component definitely improves the tracking performance of all three control strategies. It allows the system to eliminate steady state tracking errors when following a curve and it minimizes the transient response of the system to changes in curvature. More detailed experimental evaluation of the control strategies in variety of weather and road conditions is necessary.

Acknowledgment. This research has been supported by Honda R&D North America Inc., Honda R&D Company Limited, Japan, PATH MOU257 and MURI program DAAH04-96-1-0341.

References

[1] R. S. Blasi. A study of lateral controllers for the stereo drive project. Master's thesis, Department of Computer Science, University of California at Berkeley, 1997.

[2] E. D. Dickmans and B. D. Mysliwetz. Recursive 3-D road and relative ego-state estimation. *IEEE*

Transactions on PAMI, 14(2):199–213, February 1992.

[3] B. Espiau, F. Chaumette, and P. Rives. A new approach to visual servoing in robotics. *IEEE Transactions on Robotics and Automation*, 8(3):313 – 326, June 1992.

[4] Arthur Gelb *et al.* *Applied optimal estimation.* MIT Press, 1994.

[5] J. Guldner, H.-S. Tan, and S. Patwarddhan. Analysis of automated steering control for highway vehicles with look-down lateral reference systems. *Vehicle System Dynamics (to appear)*, 1996.

[6] Alberto Isidori. *Nonlinear Control Systems.* Springer Verlag, 1989.

[7] J. Košecká, R. Blasi, C.J. Taylor, and J. Malik. Vision-based lateral control of vehicles. In *Proc. Intelligent Transportation Systems Conference, Boston*, 1997.

[8] M. F. Land and D. N. Lee. Where we look when we steer? *Nature*, 369(30), June 1994.

[9] Y. Ma, J. Košecká, and S. Sastry. Vision guided navigation for a nonholonomic mobile robot. In *Proceedings of CDC'97*, 1997.

[10] Ü. Özgüner, K. A. Ünyelioglu, and C. Hatipoğlu. Steering and Lane Change: A Working System. IEEE Conference on Intelligent Transportation Systems, Boston,1997.

[11] H. Peng. *Vehicle Lateral Control for Highway Automation.* PhD thesis, Department of Mechanical Engineering, University of California, Berkeley, 1992.

[12] M. Herman, M. Nashman, T. Hong, H. Schneiderman, D. Coombs, G.-S. Young, D. Raviv and A. J. Wavering Minimalist Vision for Navigation, *Visual Navigation: From Bilogical Systems to Unmanned Ground Vehicles*, Lawrence Erlbaum Associates, 1997, edt.: Y. Aloimonos, Mahwah, New Jersey.

[13] C. J. Taylor, J. Malik, and J. Weber. A real-time approach to stereopsis and lane-finding. In *Proceedings of the 1996 IEEE Intelligent Vehicles Symposium*, pages 207–213, Seikei University, Tokyo, Japan, September 19-20 1996.

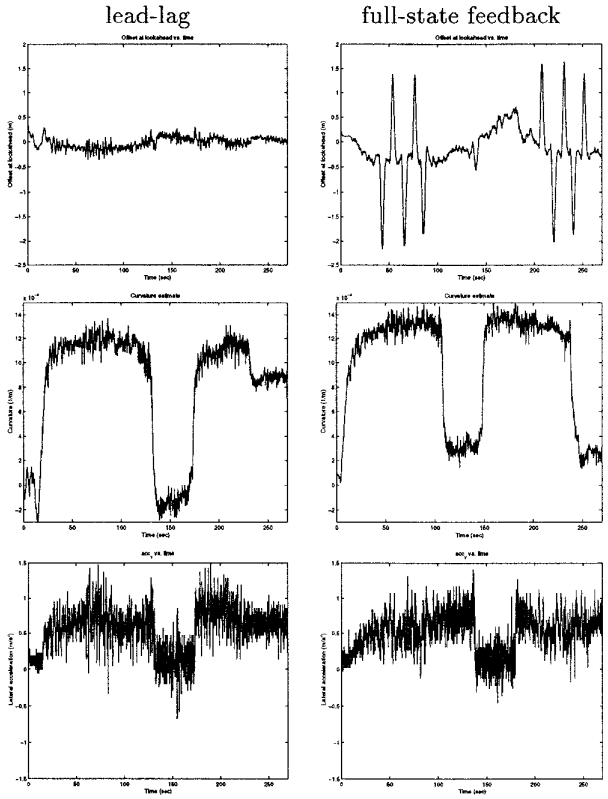

Figure 7: These plots demonstrate the effect of the feedforward control term on the overall tracking performance for two of the tested control strategies. The first row of plots indicates the tracking performance measured in terms of the offset at the lookahead, the second row depicts the curvature estimate used in the feedforward term, which was provided by the observer and the last row shows the lateral acceleration profiles. Notice that the steady state offset in the curved sections was essentially eliminated. The offset plots all exhibit a slight overshoot during transitions in curvature until the curvature estimates converge. In case of full state feedback controller the spikes in the offset measurements as well as in the lateral acceleration profile correspond to the lane change maneuvers which the vehicle performed at lower speeds.